Annual Report for the 2008 SCEC project #08059

Physical Limits on Ground Motion From Ruptures on Non-Planar Faults with Off-Fault Damage

Principal Investigators:
Steven M. Day (SDSU)
Benchun Duan (TAMU)

In this project, we first complete a study on elastoplastic dynamics of non-planar faults. In this part of the project, we examine inelastic strain distribution near a fault kink and how inelastic strain affects rupture dynamics and seismic radiation from the kink. We find that extensive inelastic deformation concentrates near a restraining bend, particularly on the side of the fault associated with rupture-front extensional strains, the deformation taking the form of a few distinct lobes and shear bands (Figure 1). The extensive inelastic deformation can reduce high-frequency radiation from the kink and the reduction is significant above several Hz (Figure 2). The calculated plastic strain distribution around the kink and the radiated pulse from the kink are nearly grid independent over the range of element size for which computations are feasible (Figures 1 and 2). We also find that plastic strain can sometimes localize spontaneously during rupture along a planar fault. However, in this case, the details of the shear banding change with numerical element size, indicating that the final plastic strain distribution is influenced by interactions occurring at the shortest numerically resolvable scales (Figure 3). This demonstrates that numerically simulating inelastic off-fault deformation is challenging. This work has been published with the SCEC contribution number of 1198:

Duan, B., and S. M. Day (2008), Inelastic strain distribution and seismic radiation from rupture of a fault kink, *J. Geophys. Res.*, 113, B12311, doi:10.1029/2008JB005847.

Then we move onto a 2D model of the Solitario Canyon fault system to address physical limits to extreme ground motion at Yucca Mountain. We start from largely reproducing the results of one model of Andrews et al. (2007): the maximum slip of 15 m case. Then we explore effects of several factors in the source region on ground motion extremes at the targeted site based on this model (supershear rupture). These factors include time-dependent pore pressure, a possible shallower dip of the fault at depths, and the presence of a possible low-velocity fault damage zone. In each case, we perform two calculations, one with elastic off-fault response and the other with elastoplastic off-fault response. Time-dependent pore pressure has obvious effects on the peak values of ground velocity at the site when off-fault materials are allowed to yielding, while it has minor effects when off-fault materials behave elastically (Figure 4). This is because pore pressure affects of-fault material strength, thus plastic yielding. This result demonstrates strong dynamic interactions among rupture on the fault, inelastic off-fault deformation, and near-field ground motion. Seismic reflection survey (Brocher et al., 1998) shows that the Solitario Canyon fault has a shallower dip at depths compared with that near the surface. Given the same seismogenic depth, the shallower dip at depths (50° versus 60°) results in a longer rupture length. This results in a significantly larger peak slip velocities at the site when off-fault response is elastic (Figure 5a). However, when off-fault response is elastoplastic, the peak velocity is only modestly higher in the vertical component, while it is even a little smaller in the horizontal

component (Figure 5b). This result may indicate that off-fault material strength dominates the peak ground motion at the site and thus place physical limits on near-field ground motion. We also examine effects of a possible low-velocity damage fault zone (100 m wide, symmetric about the fault). We find that a low-velocity fault zone introduces more high-frequency contents in ground motion at the site with either elastic or elastoplastic off-fault response (Figure 6). This work was presented in the ExGM workshop and the SCEC Annual meeting in September 2008 as follows:

Duan, B., and S. M. Day, Sensitivity of ground motion at Yucca Mountain to uncertainties in fault geometry and fault zone structure, ExGM workshop, Palm Springs, CA, September 6, 2008 (Invited talk).

Duan, B., and S. M. Day, Sensitivity of ground motion at Yucca Mountain to uncertainties in fault geometry and fault zone structure, SCEC Annual Meeting, Palm Springs, CA, September 6-11, 2008 (Poster).

We plan to perform another group of simulations with subshear rupture and to write a manuscript on this work in Year 2009.

References

Andrews, D. J., T. C. Hanks, and J. W. Whitney (2007), Physical limits on ground motion at Yucca Mountain, *Bull. Seismol. Soc, Am.*, 97, 1771-1792, doi:10.1785/0120070014.

Brocher, T. M., W. C. Hunter, and V. E. Langenheim (1998), Implications of seismic reflection and potential field geophysical data on the structural framework of the Yucca Mountain-Crater Flat region, *GSA Bulletin*, v. 110, no. 8, 947-971.

Duan, B., and S. M. Day (2008), Inelastic strain distribution and seismic radiation from rupture of a fault kink, *J. Geophys. Res.*, 113, B12311, doi:10.1029/2008JB005847.

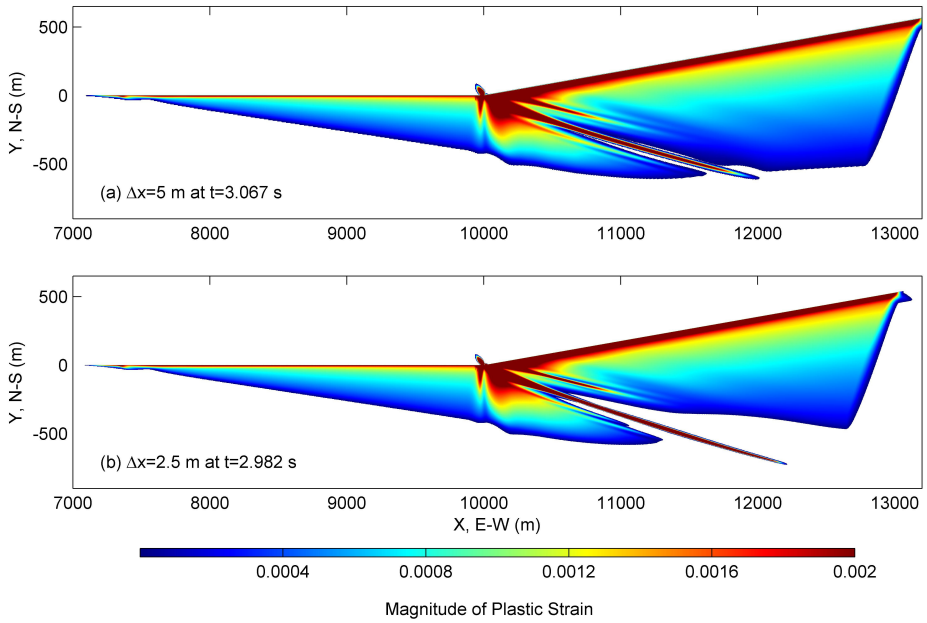

Figure 1. Distribution of off-fault plastic strain magnitude due to rupture on a fault with a kink (at x = 10 km, y = 0 km). Plastic strain localizes into bands and lobes near the kink, and the solution of the localization is apparently convergent when the element size is reduced. (From Duan and Day, 2008).

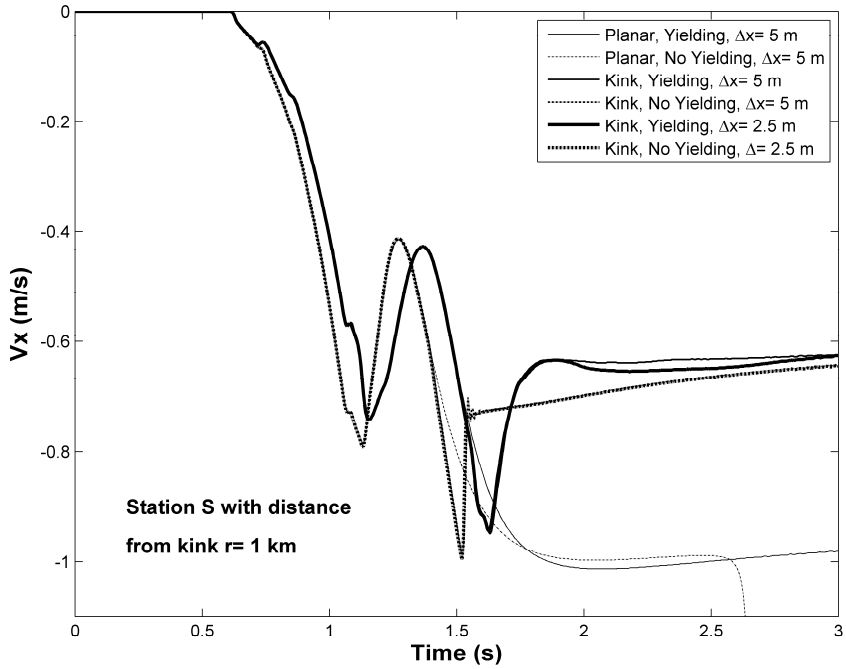

Figure 2. Particle velocity time histories from six simulations. Velocity jumps beyond 1.5 s from the kink fault model are caused by seismic radiation from the kink. Plastic yielding near the kink reduces high-frequency radiation from the kink (indicated by a larger rise time). (After Duan and Day, 2008).

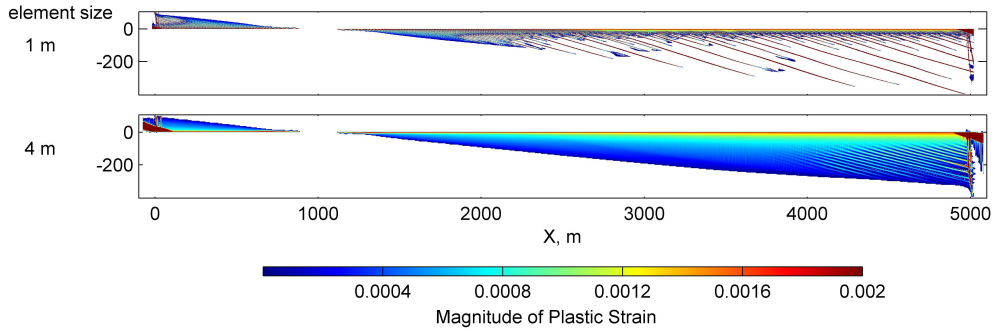

Figure 3. The distribution of plastic strain magnitude in a planar fault model with two different element sizes. Features of plastic strain localization keep changing with the element size, imposing a challenging in numerically simulating the localization. (From Duan and Day, 2008).

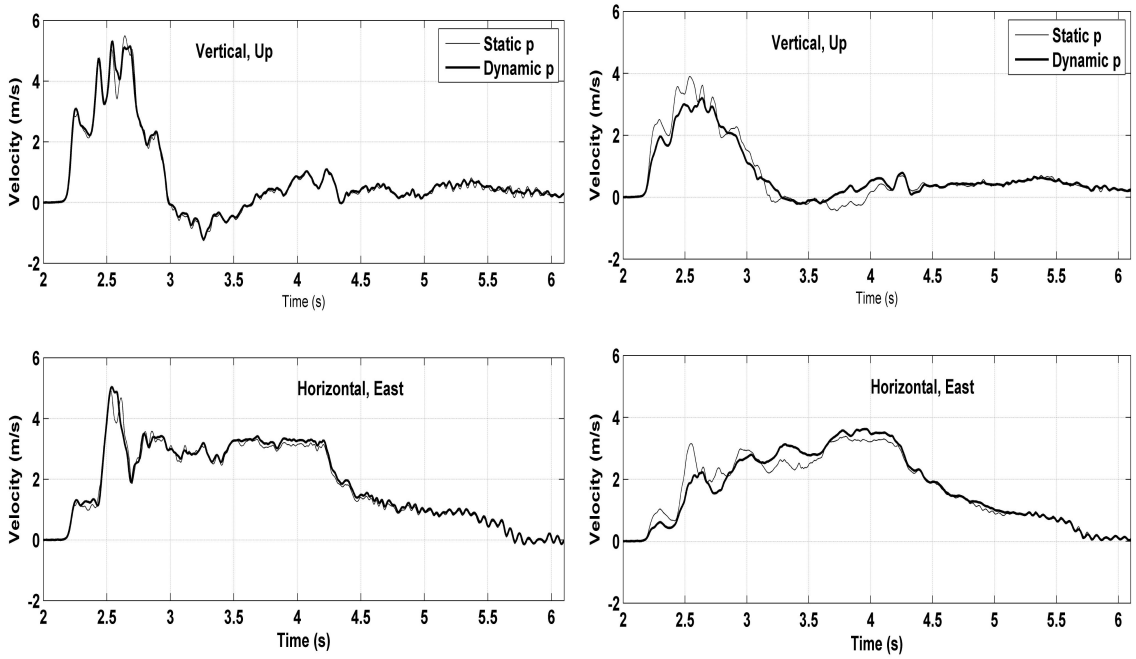

Figure 4. Time-dependent pore pressure (dynamic p) effects on ground motion (vertical and horizontal velocities) at the Yucca Mountain site from a model of elastic off-fault response (a) and a model of elastoplastic off-fault response (b). The reference case (static p) assumes a constant pore pressure at a point in the models during the dynamic events. Time-dependent pore pressure has obvious effects on peak ground velocities when off-fault material yields (b).

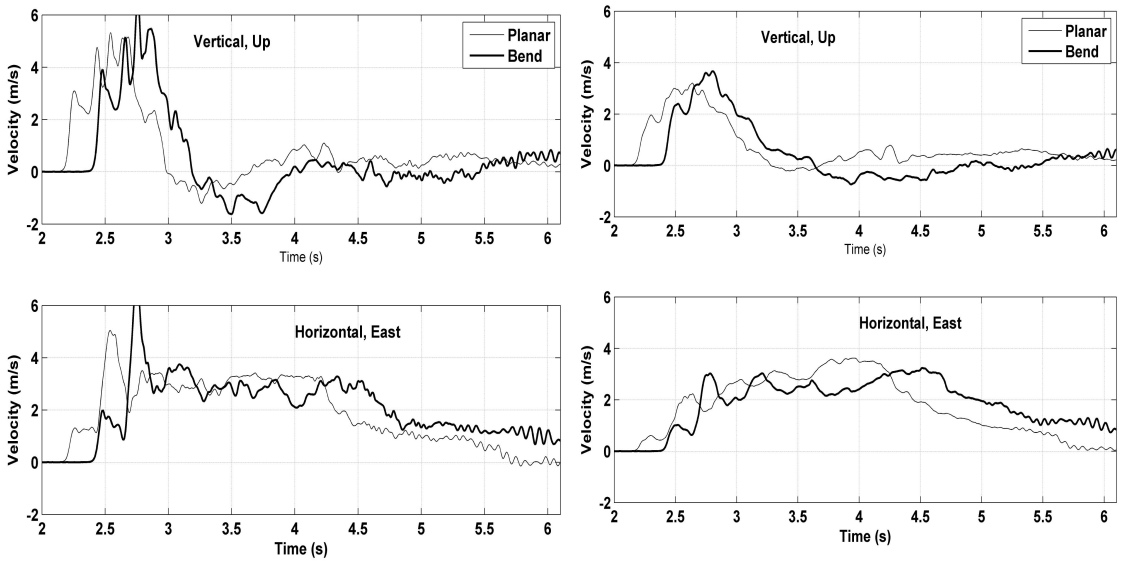

(a) (b)

Figure 5. Fault geometry effects on ground motion at the Yucca Mountain site from a model with off-fault elastic response (a) and a model with off-fault elastoplastic response (b). 'Planar' denotes a normal fault with a constant dip of 60, and 'Bend' represents the fault has a change in dip at 1 km depth from 60 near the surface to 50 at depths. Effects are significant when off-fault material behaves elastically (a).

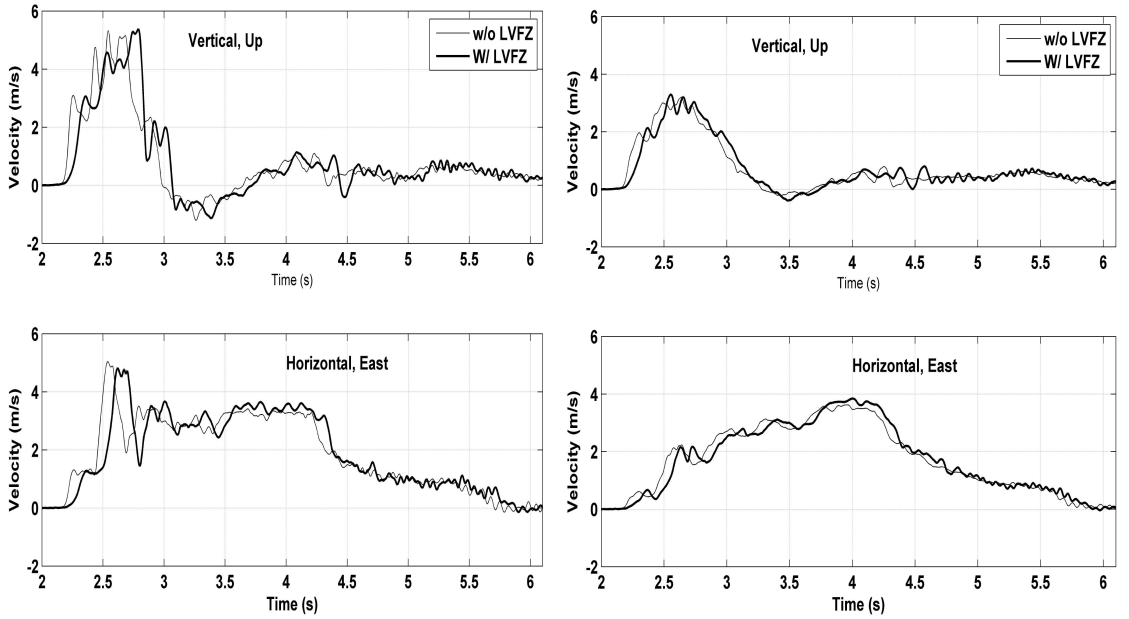

(a) (b)

Figure 6. Effects of a low-velocity fault zone (LVFZ) on ground motion at the Yucca Mountain site from a model with off-fault elastic response (a) and a model with off-fault elastoplastic response (b). The LVFZ has a width of 100 m and the planar fault bisects the fault zone. In both (a) and (b), more high-frequency contents can be observed with the presence of LVFZ.